Journal of Mechanical and Electrical Intelligent System (JMEIS)

Leak-Before-Break and Plastic Collapse Strength Evaluation of Stainless Steel Piping with a Part-Through Notch by Using Double-Elastic-Deformation Method

Masato Ogawa[1,a], Masaaki Matsubara[1,b] and Ryosuke Suzuki[1,c,*]

[1]Graduate School of Science and Technology, Gunma University 1-5-1, Tenjin-cho, Kiryu, Gunma 376-8515, Japan

*Corresponding author

[a]<t181b015@gunma-u.ac.jp>, [b]<m.matsubara@gunma-u.ac.jp>, [c]<r_suzuki@gunma-u.ac.jp>

Keywords: stainless steel pipe, integrity assessment, leak-before-break, plastic collapse strength, DED method.

Abstract. Nuclear power plants and chemical plants contain many piping, which degrades with age. As a result of a reduction in structural strength, guillotine breaking and rupturing can occur. Piping is subjected to tension and bending, but the influence of the load history on the integrity of piping is poorly understood. The present study is to develop an improved integrity assessment method for a stainless steel pipe with a part-through notch that takes into account the load history. This involved: (1) Determining the feasibility of the leak-before-break (LBB) concept for piping, (2) Evaluating the crack penetration stress and (3) Estimating the plastic collapse strength. Conclusions are as follows: (1) The LBB concept is found to be applicable, (2) The crack penetration stress is approximately equal to the maximum stress and (3) The plastic collapse strength of a part-through notched specimen can be safely estimated using the theoretical plastic collapse strength of a through-wall notched pipe.

1. Introduction

Piping is widely used in fields related to energy storage, such as nuclear power plants. There are several types of nuclear reactors [1], and many of the nuclear power plants in Japan are light-water reactors. Steam is generated by a light-water reactor using low-enriched uranium as fuel and turns a turbine to create electricity. Piping for transporting steam to the turbine and for transporting cooling water is generally constructed from an austenitic stainless steel, which has excellent ductility, toughness, and corrosion resistance. High-temperature and high-pressure fluid flows in the piping, which is always subjected to tensile stress in the axial direction and the circumferential direction due to the internal pressure [2, 3]. Damage such as fatigue cracking, thinning, and stress corrosion cracking is caused by aging. In addition, cracks leading to failure occur in the piping when the piping is accidentally subjected to the high stresses caused by earthquakes. The load history of the tension caused by the internal pressure and the bending load due to the earthquake is not clear in actual piping [4, 5]. Therefore, it is necessary to investigate the influence of the load history on the integrity of piping. The integrity assessment is carried out based on the Rules on Fitness-for-Service for Nuclear Power Plants (maintenance standard) of the Japan Society of Mechanical Engineers in Japan [6]. If flaws are found in the piping at a nuclear power plant, they are modeled in a form that enables the integrity of the piping to be evaluated using fracture mechanics. Then, whether the model of the flaw is within the allowable size range is judged.

The LBB concept is a fail-safe design criterion and is especially important for the nuclear industry [7]. In the LBB concept, a significant crack can be detected before a guillotine break because fluid leaks through the crack from piping before unstable fracture occurs. A guillotine break in piping can cause severe damage to a nuclear power plants. The validity of the LBB concept considering the load history has not been sufficiently discussed. The present study attempts to clarify the influence of load

history on the validity of LBB for cracked austenitic stainless steel pipe subjected to a combined load of tension and bending, and the following topics are investigated. A combined load of tension and bending is applied to pressurized austenitic stainless steel piping having a part-through notch until failure, and the plastic collapse stress, the stress at the leakage, and the maximum stress are discussed.

2. Theory

The theoretical plastic collapse stress is calculated for a pipe with a circumferential part-through notch. The distribution of the stress along the axial direction in the ligament area of a part-through notched pipe subjected to a combined axial force F and bending moment M at plastic collapse is shown in Fig. 1.

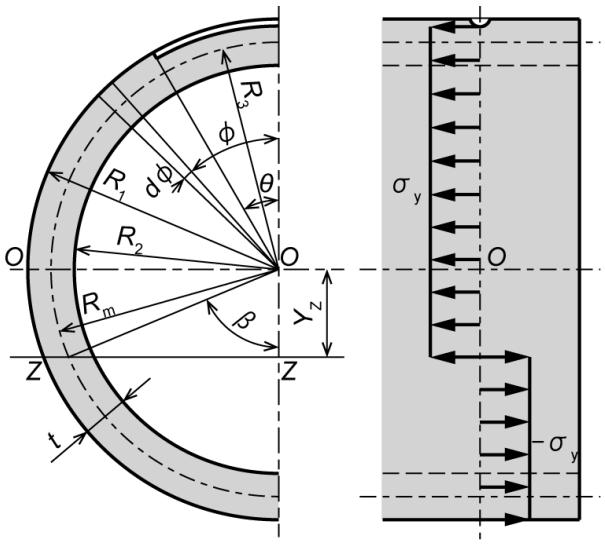

Fig. 1. Stress distribution of piping with a circumferential part-through notch.

The pipe is assumed to be a thin-walled cylinder and an elastic-perfectly plastic body to calculate the theoretical plastic collapse stress. The relationship between the membrane stress, σ_m, and the bending stress, σ_b, for the part-thorough notched pipe at plastic collapse can be obtained from the following equations:

$$\frac{\sigma_b}{\sigma_y} = \frac{2tR_m\{2R_m \sin\beta - R_m \sin\theta + |Y_z|(\pi-\theta-2\beta)\}}{Z_e} + \frac{(R_3-R_2)(R_3+R_2)\left(\frac{R_3+R_2}{2}\sin\theta + |Y_z|\theta\right)}{Z_e} \tag{1}$$

$$\beta = \frac{1}{4tR_m}\{2tR_m(\pi-\theta) + (R_3-R_2)(R_3+R_2)\theta\}\left(1-\frac{\sigma_m}{\sigma_y}\right) \tag{2}$$

$$\frac{\sigma_m}{\sigma_y} = \frac{2tR_m(\pi-\theta-2\beta)+(R_3-R_2)(R_3+R_2)\theta}{2tR_m(\pi-\theta)+(R_3-R_2)(R_3+R_2)\theta} \tag{3}$$

$$I_z = tR_m^3\left(\pi-\theta-\frac{1}{2}\sin 2\theta\right) + \frac{1}{8}(R_3+R_2)^3(R_3-R_2)\left(\theta+\frac{1}{2}\sin 2\theta\right) - \left(\frac{-2tR_m^2\sin\theta+\frac{1}{2}(R_3+R_2)^2(R_3-R_2)\sin\theta}{2tR_m(\pi-\theta)+(R_3-R_2)(R_3+R_2)\theta}\right)^2 \{2tR_m(\pi-\theta)+(R_3-R_2)(R_3+R_2)\theta\} \tag{4}$$

$$Z_e = \frac{I_z}{R_3 + |Y_z|} \tag{5}$$

where θ is the half notch angle, R_m is the average radius of the pipe, R_1 is the outer radius of the pipe, R_2 is the inner radius of the pipe, R_3 is the curvature radius of the bottom of notch, Y_z is the distance from the center to the centroid of the cross-section of the ligament, Z_e is the section modulus in the ligament section, t is the pipe wall thickness, and σ_y is the yield stress of the pipe material. The theoretical plastic collapse limit curve of an austenitic stainless-steel pipe with a circumferential part-through notch having a notch angle of 90° is shown in Fig. 2. The theoretical plastic collapse limit curve is used to determine the loading paths for the experiments and to evaluate the experimental plastic collapse stress and maximum stress.

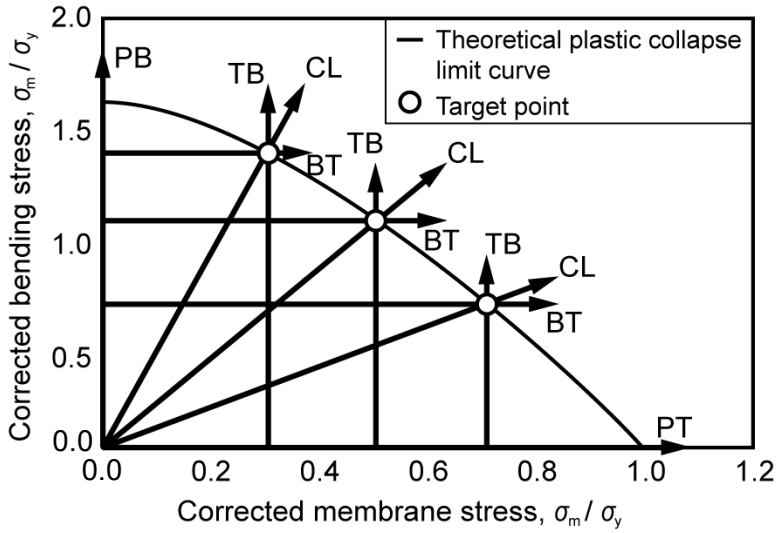

Fig. 2. Loading patterns through the target points for the part-through notched specimens.

3. Experiment

3.1 Specimen

An austenitic stainless steel pipe (SUS 304) was used as a specimen. A schematic diagram of the specimens is shown in Fig. 3, and the mechanical properties are listed in Table 1. The specimen has a length of 110 mm, a diameter of 32.0 mm, and a thickness of 3.0 mm. A part-thorough notch with a depth of 1.5 mm and a notch angle of 90° was cut into the center of the specimen by wire electric discharge machining. Another type of specimen with a through-wall notch having a notch angle of 90° was made for comparison. The notch tip radius was 0.16 mm, and the notch width was 0.32 mm. The jigs were welded to both ends of the specimens. A schematic diagram of the specimen with the jigs is shown in Fig. 4. An air valve was attached to a jig, and a pressure gauge was attached the other jig. The part-through notched specimen was subjected to internal air pressure. The internal air pressure in the specimen was measured using a pressure gauge. The internal pressure decreased due to air leaking from the specimen when the crack extended from the notch tip to the inside of the pipe wall. The stress at the crack penetration point can be obtained as the stress at the air-leakage point.

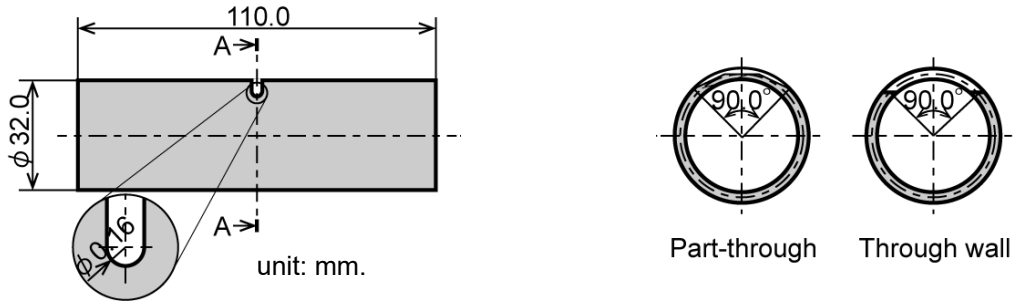

(a) The specimen (austenitic stainless steel pipe) (b) Two types of A-A cross section area

Fig. 3. A part-through notched specimen and a through-wall notched specimen.

Table 1. Mechanical properties of the pipe material.

Yield stress [σ_y/MPa]	Ultimate tensile strength [σ_u/MPa]
262	606

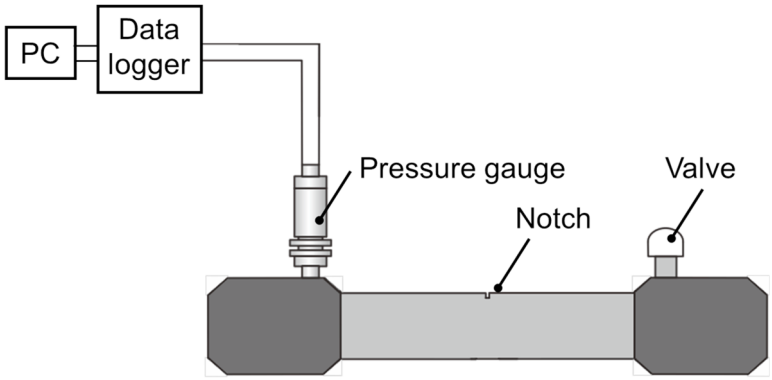

Fig. 4. Specimen setup.

3.2 Testing Equipment

Loading tests were carried out using statically indeterminate fracture mechanics testing equipment developed by our university [8]. A photograph and schematic diagram of the testing equipment are shown in Figs. 5 and 6, respectively. A load cell, a displacement gauge, and an actuator are installed in both the axial direction and the vertical direction in the testing equipment. The deflection angle is measured with two displacement gauges on top of the specimen. The testing equipment can apply arbitrary sequences of tension and bending to the specimen. The loading test can be carried out considering the load history by using this testing equipment.

Both ends of the specimen are attached to the horizontal actuator and a horizontal load cell via the jig. A bending moment is applied to the specimen by four-point bending. The distances between the inner supports and between the outer supports are 70 mm and 384 mm, respectively. A roller is installed at the tip of inner support in order to prevent the influence of a frictional force caused by the friction between the specimen and the inner supports during the loading test.

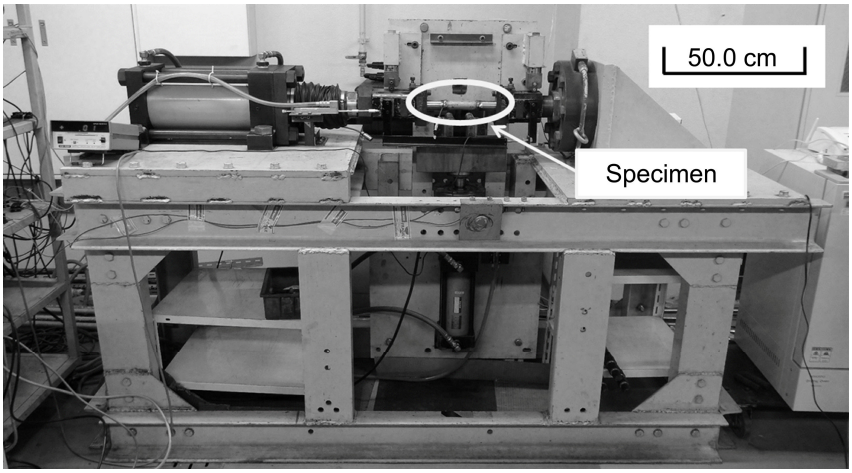

Fig. 5. Photograph of the testing equipment for statically indeterminate fracture.

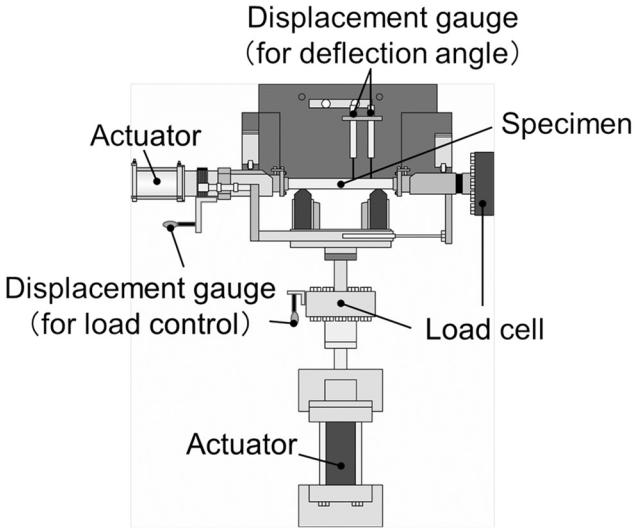

Fig. 6. Schematic diagram of the testing equipment for statically indeterminate fracture mechanics.

3.3 Procedures

The tests were carried out under the following five load conditions through the target point, σ_m/σ_y, on the theoretical plastic collapse limit curve Fig. 2.

(1) concurrent loading (CL),
(2) tensile load followed by bending load (TB),
(3) bending load followed by tensile load (BT),
(4) pure tension (PT), and
(5) pure bending (PB).

The loading conditions of CL, TB and BT were determined with σ_m/σ_y = 0.3, 0.5 and 0.7 as target points on the theoretical plastic collapse limit curve.

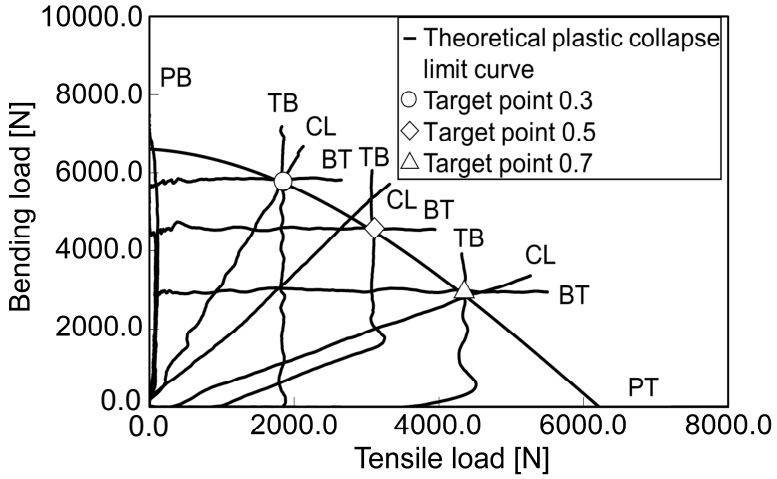

Fig. 7. Load paths of the part-through notched specimen.

The stress-displacement diagrams and the stress-deflection diagrams were made and the plastic collapse stress was obtained from the load-displacement diagrams using the double elastic deformation (DED) method [9,10]. The experimental plastic collapse stress of a part-through notched specimen is compared with the theoretical plastic collapse stress and the experimental plastic collapse stress of a through-wall notched specimen.

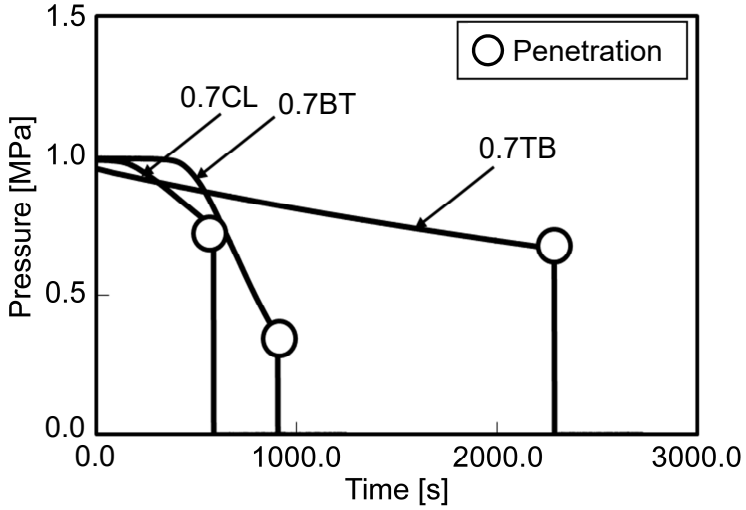

Fig. 8. Internal pressure-time curve.

The vertical and horizontal loads when the internal pressure began to decrease were used to calculate the membrane stress and bending stress at the crack penetration point. The crack penetration point was used to evaluate the validity of LBB. If the crack penetration stress occurs before the maximum stress, then the LBB is valid.

4. Results and Discussion

The actual loading paths are shown in Fig. 7. The arbitrary combined axial tensile and bending loads can be applied to the specimens through the target point using the developed test equipment. The internal pressure-time diagrams at the target point 0.7 and the loading paths for the CL, TB, and BT tests as typical pressure-time diagrams, are shown in Fig. 8. The abrupt lowering point of the internal

pressure was observed for all testing conditions. The crack reached the inside of the pipe wall at the abrupt lowering point of the internal pressure. The internal pressure was slightly decreased before notch penetration because the internal volume of the specimen increased due to the loading test

The membrane stress-axial displacement diagrams of the part-through notched specimen and the through-wall notched specimen for the 0.7 CL and 0.7 BT tests, as typical results, are shown in Figs. 9 and 10. The bending stress-deflection angle diagram for the 0.7 TB test is shown in Fig. 11, as a typical result. The plastic collapse strengths of the through-wall notched specimen and the part-through notched specimen are obtained from the above diagrams using the DED method. In Figs. 9, 10, and 11, ○, □, and ◇ indicate the plastic collapse points determined by the DED method, the crack penetration points, and the maximum stress points, respectively.

The plastic collapse strength of the part-through notched specimen was close to that of the through-wall notched specimen, and the average error between the plastic collapse strengths was less than 10%. The plastic collapse strength of the part-through notched specimen could be estimated using the plastic collapse strength of the through-wall notched specimen under all test conditions.

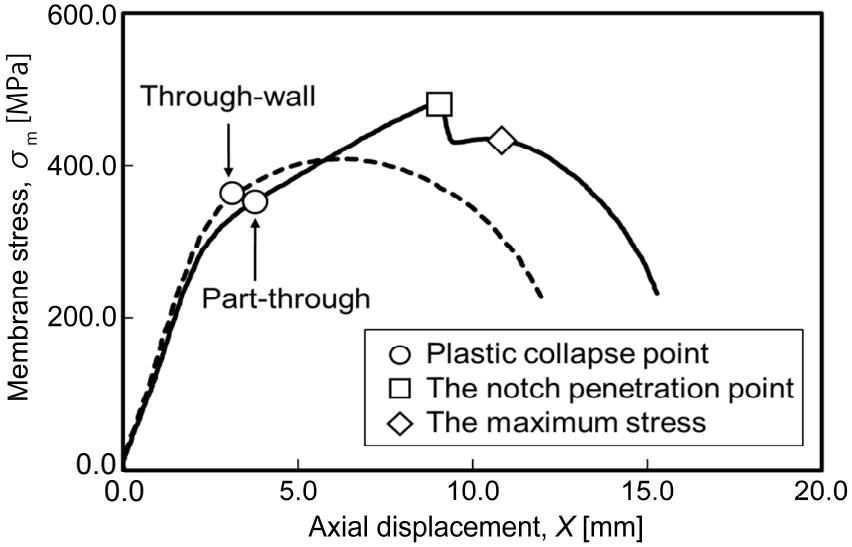

Fig. 9. Plastic collapse stress of through-wall and part-through notched specimens in the CL test (target point: 0.7).

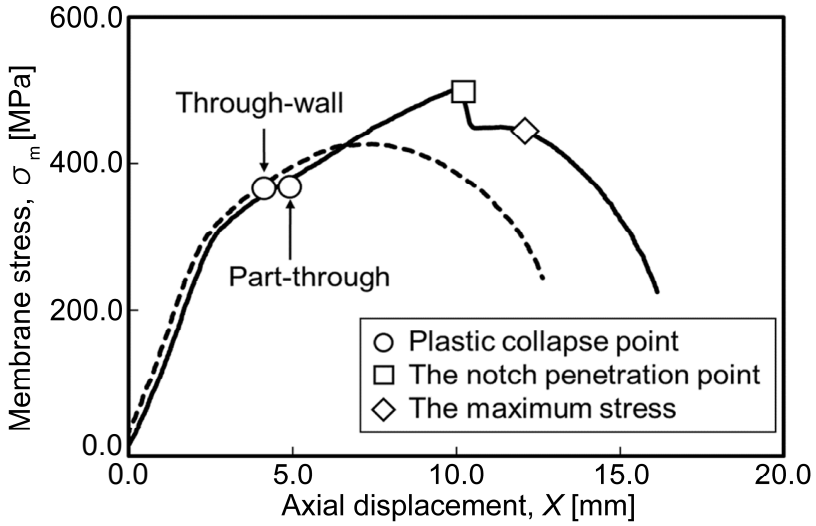

Fig. 10. Plastic collapse stress of through-wall and part-through notched specimens in BT test (target point: 0.7).

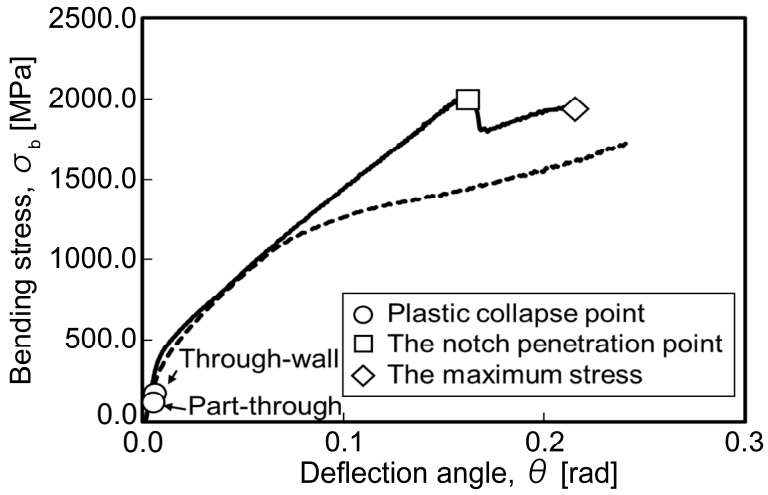

Fig. 11. Plastic collapse stress of through-wall and part-through notched specimens in the TB test (target point: 0.7).

The membrane stress and bending stress of the part-through notched specimen decreased rapidly at the crack penetration point and increased for all loading conditions. Thus, LBB is valid under the combined tensile force and bending conditions considered in the present study because the crack penetration occurred in the stable fracture region.

The stress at the crack penetration point (penetration stress) of the part-through notched specimen is compared with the maximum stress after the crack penetration under each loading condition (Table 2). The following equation was used for calculation of the error value x:

$$x = \frac{|\sigma_P - \sigma_M|}{\sigma_P} \tag{6}$$

Table 2. Penetration stress and maximum stress after crack penetration of the part-through notched specimen.

	Penetration stress, σ_P [MPa]	Maximum stress, σ_M [MPa]	Error, x [%]
0.3CL	1831	1668	8.87
0.5CL	1115	1116	0.05
0.7CL	482	436	9.58
0.3BT	498	443	10.88
0.5BT	492	468	4.84
0.7BT	500	450	9.99
0.3TB	1320	1234	6.52
0.5TB	1457	1546	6.08
0.7TB	1962	1948	0.81
PT	501	475	5.06
PB	877	749	11.55

The penetration stress is close to the maximum stress after crack penetration, and the error between both stresses is less than 10% under most loading conditions. Therefore, the stress at the crack penetration point can be estimated using the same estimation formula of the maximum stress after crack penetration.

The penetration stress is estimated using the following estimation formula for the maximum stress:

$$\sigma_{zm} = 1.9\sigma_y + (1 - \sigma_m/\sigma_y)\ \sigma_y \tag{7}$$

$$\sigma_{zb} = 3.2\sigma_f - (1 - \sigma_m/\sigma_y)(\sigma_b/\sigma_y)\sigma_f \tag{8}$$

where σ_f is the flow stress, which is the average of the yield stress and the tensile strength (Table 1). The penetration stress is plotted in Fig. 12, and theoretical plastic collapse limit curve and the estimation curve of the part-through notched specimen are also plotted in Fig. 12. The penetration stress is larger than the theoretical plastic collapse stress. On the other hand, the penetration stresses are distributed approximately along the estimation curve. Therefore, the penetration stress of the part-through notched specimen can be approximated using the estimation formula of the maximum stress under the loading conditions considered in the present study.

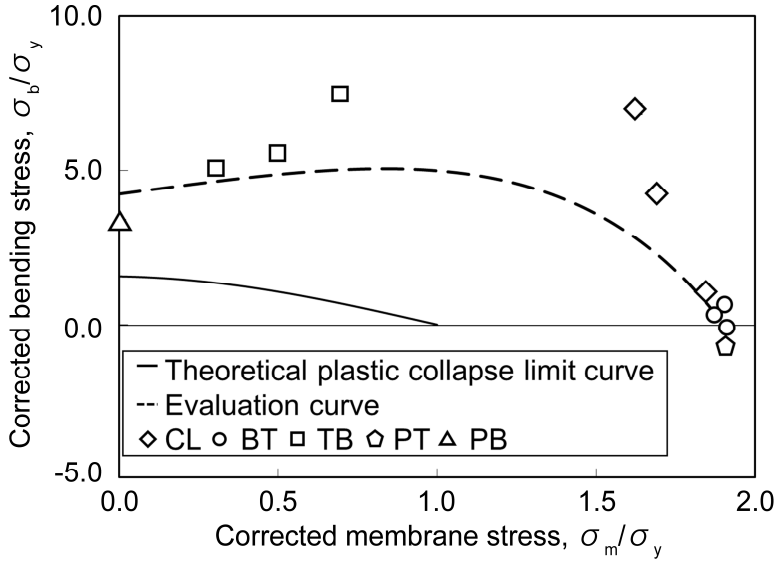

Fig. 12. Estimation for the penetration stress of part-through notched specimens.

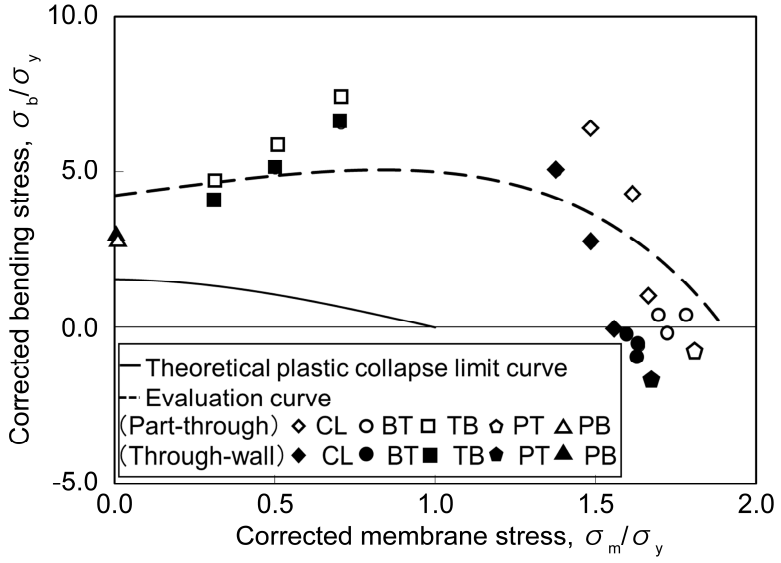

Fig. 13. Maximum stress estimation of through-wall notched specimens and part-through notched specimens.

The maximum stresses of the through-wall notched specimen and the part-through notched specimen are plotted in Fig. 13. The theoretical plastic collapse limit curve and the estimation curve for the maximum stress of the part-through notched specimen are also shown in Fig. 13. The maximum stress of the part-through notched specimen is dispersed slightly outside that of the through-wall notched specimen under most loading conditions because the ligament area of the part-through notched specimen is larger than that of the through-wall notched specimen. On the other hand, both maximum stresses are dispersed approximately along the evaluation curve. Therefore, the maximum stress of the part-through notched specimen can be approximated using the same estimation formula of the maximum stress under the loading conditions of the present study.

5. Conclusions

In order to clarify the influence of load history on the validity of LBB for cracked austenitic stainless steel pipe subjected to a combined load of tension and bending, combined loading tests of axial force and bending were performed on stainless steel pipe with a single circumferential part-through notch with a notch angle of 90° and a notch depth of 50% of wall thickness. As a result, the following conclusions were obtained.

1) The LBB concept is valid for austenitic stainless steel pipe with a single circumferential part-through notch with a notch angle of 90° and a notch depth of 50% of wall thickness under all loading conditions.

2) The penetration stress of the part-through notched specimen was approximately equal to the maximum stress after crack penetration and can be approximated using the estimation formula for the maximum stress.

3) The plastic collapse strength and the maximum stress of a part-through notched pipe can be approximated using the plastic collapse strength and maximum stress of a through-wall notched pipe having the same notch angle.

References

[1] R. Suzuki, M. Matsubara, S. Yanagihara, M. Morijiri, A. Omori and T. Wakai, “Collapse evaluation of double notched stainless pipes subjected to combined tension and bending”, ***Procedia Materials Science***, Vol. 12, pp.24-29, 2016.

[2] S. Izawa and M. Matsubara, “Plastic collapse of a notched austenitic stainless steel specimen under combined tension and bending”, ***Transactions of the JSME***, Vol. 73, No. 728, pp.537-543, 2007.

[3] H. Okamura, K. Watanabe and T. Takano, “Deformation and strength of cracked member under bending moment and axial force”, ***Engineering Fracture Mechanics***, Vol. 7, No. 3, pp.531-539, 1975.

[4] S. Izawa, M. Matsubara, K. Nezu and K. Sakamoto, “Plastic collapse evaluation on the notched stainless steel piping subjected to combined tension and bending by photo-elastic coating”, ***Key Engineering Materials***, Vol. 270–273, pp. 2001-2005, 2004.

[5] S. Izawa, M. Matsubara, N. Hirao, K. Busujima, T. Koyama, K. Machida, D. Kawada, A. Ohta and H. Harizuka, “Combined tension-bend system for large deformation analysis”, ***Experimental Techniques*****,** Vol.31, No. 5, pp.42-45, 2007.

[6] Codes for Nuclear Power Generation Facilities - Rules on Fitness-for-Service for Nuclear Power Plants- JSME S NA1-2008, The Japan Society of Mechanical Engineers (Tokyo, Japan), 2008.

[7] Cods for Nuclear Power Generation Facilities -Rules on Protection Design against Postulated Pipe Rupture for Nuclear Power Plants- JSME S ND 1-2002, The Japan Society of Mechanical Engineers (Tokyo, Japan), 2002.

[8] M. Matsubara, S. Izawa, N. Hirao, K. Busujima, T. Koyama, K. Machida, D. Kawada, K. Sakamoto and K. Nezu, "Development of a testing equipment for studying statically indeterminate fracture mechanics", ***Proceedings ICPVT-10*** (Veinna, Austria), July 2003.

[9] S. Saxena and N. Ramakrishnan, "Characterization of plastic collapse load determination in circumferentially through-wall cracked elbows", ***Nuclear Engineering and Design***, Vol. 236, No. 17, pp.1739-1747, 2006.

[10] R. Suzuki, M. Matsubara, K. Sakamoto, M. Suzuki, T. Shiraishi, S. Yanagihara, S. Izawa and T. Wakai, "Observation and evaluation of plastic collapse for double-notch pipe", ***Experimental Techniques***, ext.12061, 2013.